Development of Bismuth Ferrite-Reinforced Bioactive Glass Scaffolds with Improved Osteogenic and Biofunctional Properties for Bone Regeneration

Sharun Khan[1,2], Amitha Banu Shajahan[1,2], Hasanur Rahaman[3,4], Merlin Mamachan[1], Swapan Kumar Maiti[1], Amar Pal[1], Subhadip Bodhak[3,4], Vamsi Krishna Balla[3,4] , Abhijit Pawde[1]

[1]Division of Surgery, ICAR-Indian Veterinary Research Institute, Izatnagar, Bareilly, Uttar Pradesh, India
[2]Regenerative Medicine Group, Department of Health Science and Technology, Aalborg University, Gistrup, 9260, Denmark
[3]Biomaterials and Medical Devices Division, CSIR-Central Glass and Ceramic Research Institute, Kolkata-700032, India
[4]Academy of Scientific and Innovative Research (AcSIR), Ghaziabad- 201002, India

TERMIS EU-Chapter 2026 PALMA DE MALLORCA 21-24 APRIL / SPAIN

termis EUROPE

Abstract
P-159

BACKGROUND AND PURPOSE

Bone tissue engineering (BTE) has emerged as a promising strategy to address the growing clinical demand for effective therapies to repair or replace damaged bone tissue arising from trauma, congenital defects, infection, and degenerative diseases. Recent advances in smart biomaterials have highlighted the importance of incorporating biophysical cues, in addition to biochemical signals, to more closely replicate the native bone environment. Bismuth ferrite has previously demonstrated potential to enhance cell proliferation, mineralization, and bioactivity when incorporated into bioactive glass systems. The purpose of the present study was to fabricate and evaluate porous bioactive glass scaffolds reinforced with low concentrations of bismuth ferrite (0.5 and 1.5 wt%) and to investigate their suitability for bone tissue engineering applications.

METHODS

Porous scaffolds of pure BAG and BAG-BF composites containing 0.5 and 1.5 wt% BF were fabricated using the foam replication technique. Material characterization was carried out using XRD for phase analysis, FTIR for functional group identification, and SEM-EDX for microstructural and elemental analysis. *In vitro* bioactivity was evaluated by immersing scaffolds in simulated body fluid for up to 21 days under a 200 mT magnetic field, with apatite formation examined using SEM-EDX. Cytocompatibility and cell proliferation were assessed using MC3T3-E1 pre-osteoblast cells through LIVE/DEAD staining and MTT assays under both magnetic field and non-field conditions. Antibacterial activity against *S. aureus* and *E. coli* was evaluated using microbial inhibition and disk diffusion assays. Hemocompatibility was assessed using an *in vitro* hemolysis test with rat RBCs.

RESULTS

X-ray diffraction revealed that the BAG component retained its amorphous nature after sintering, while BF preserved its crystalline $BiFeO_3$ phase, indicating phase stability and compatibility between the two components. SEM and EDX analyses further confirmed the uniform, isolated dispersion of BF particles within the glass matrix, without agglomeration, which is critical for ensuring consistent electroactive behavior. The measured porosities were approximately 74% for pure BAG, 65% for 0.5 wt% BF-reinforced BAG, and 64% for 1.5 wt% BF-reinforced BAG, with pore sizes ranging from 400 to 500 µm. The compressive strength of pure BAG scaffolds was measured at 1.45 MPa, which increased to 1.81 MPa (approximately 29% improvement) for 0.5 wt% BAG-BF and 1.87 MPa (approximately 33% improvement) for 1.5 wt% BAG-BF.

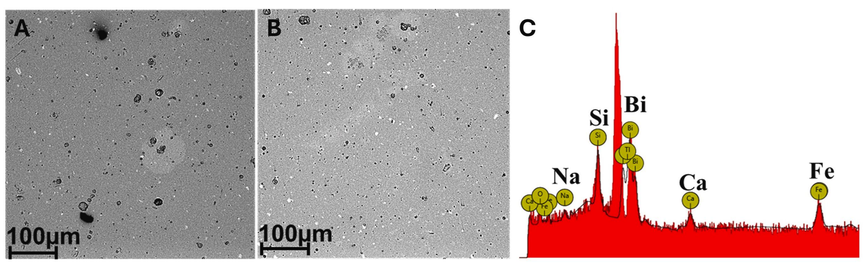


Fig. 1. Typical micrographs of sintered BAG-BF composites (A) 0.5 BAG-BF and (B) 1.5 BAG-BF reveal the dispersion of BF (bright phase) within the BAG matrix (grey phase) along with the presence of porosity (black spherical features), (C) EDX spectrum showing the presence of different elements in the composites.

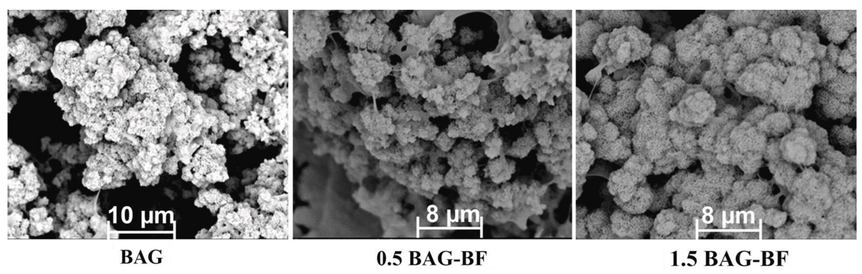
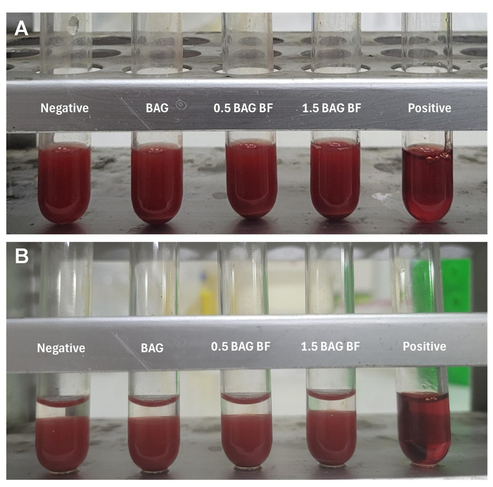


Fig. 6. The typical surface morphology of porous samples showing the formation of apatite precipitates after 21 days of immersion in SBF, with 200 mT magnetic field exposure for 30 min per day. (A) BAG (B) 0.5 BAG-BF (C) 1.5 BAG-BF.



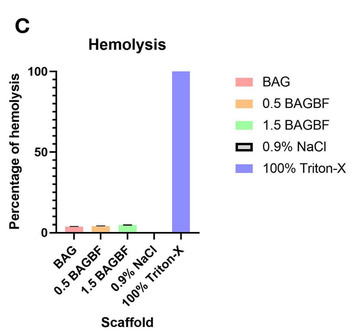


Fig. 9. *In vitro* hemolysis of scaffolds (A) before and (B) after 1 h incubation. BAG, 0.5 BAG-BF, and 1.5 BAG-BF exhibited mild hemolytic effects (3.8 %, 4.21 %, and 4.83 %, respectively), while the negative control (0.9 % NaCl) showed no hemolysis.

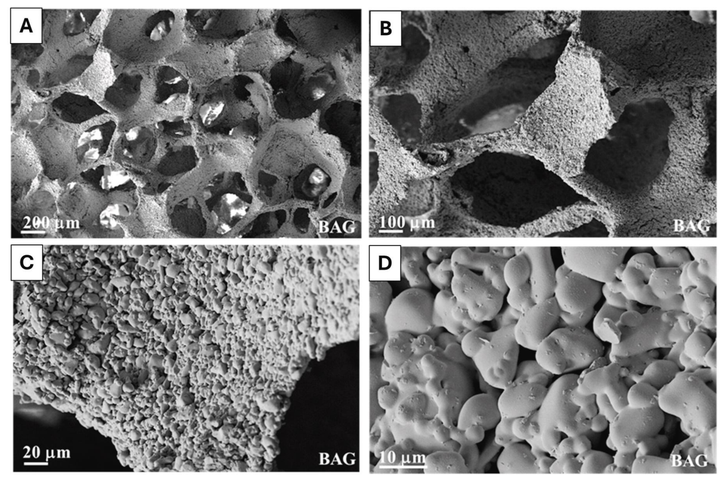


Fig. 4. The surface morphology of the BAG porous scaffolds, at different magnifications, showing highly interconnected porosity and sintered BAG powder in the struts with rough surface morphology.

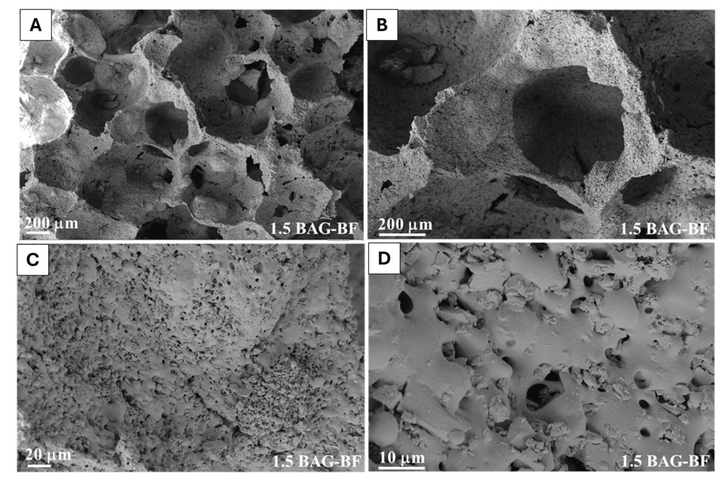


Fig. 5. The surface morphology of the 1.5 BAG-BF porous scaffolds, at different magnifications, showing highly interconnected porosity and relatively denser struts than observed in BAG scaffolds with rough surface morphology.

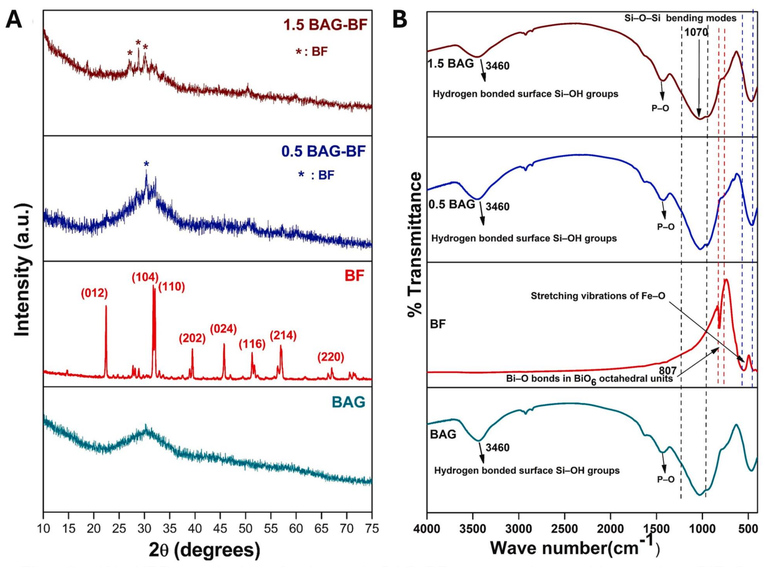


Fig. 2. (A) XRD analysis of sintered BAG-BF composites with varying $BiFeO_3$ concentrations, showing phase evolution. (B) FTIR spectrum of the sintered samples, highlighting the vibrations associated with different functional groups in the composites.

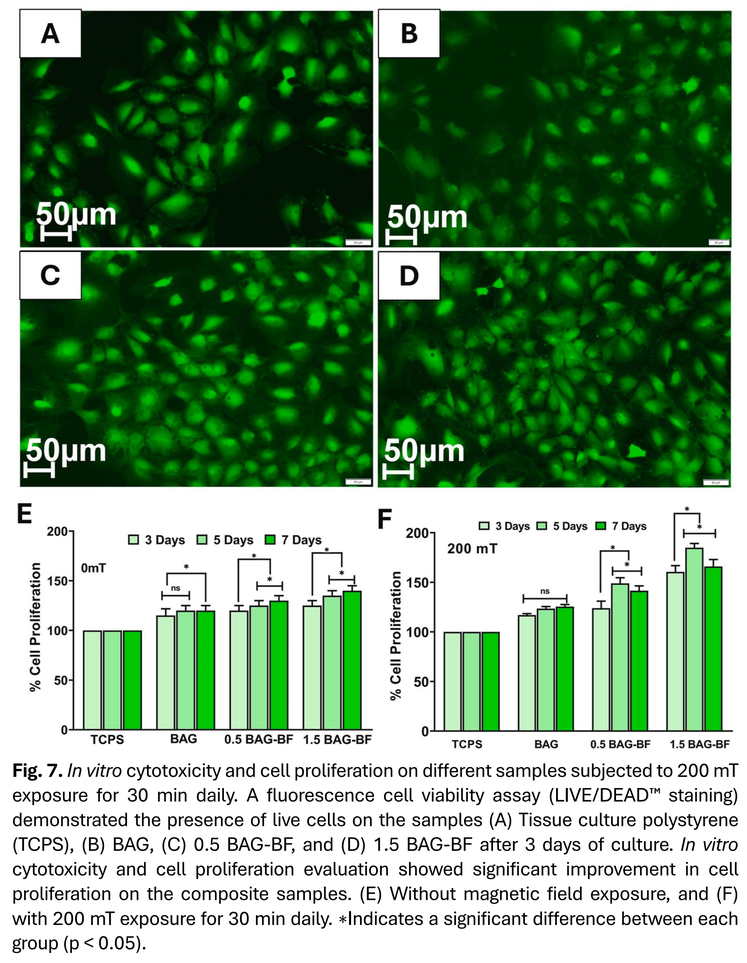


Fig. 7. *In vitro* cytotoxicity and cell proliferation on different samples subjected to 200 mT exposure for 30 min daily. A fluorescence cell viability assay (LIVE/DEAD™ staining) demonstrated the presence of live cells on the samples (A) Tissue culture polystyrene (TCPS), (B) BAG, (C) 0.5 BAG-BF, and (D) 1.5 BAG-BF after 3 days of culture. *In vitro* cytotoxicity and cell proliferation evaluation showed significant improvement in cell proliferation on the composite samples. (E) Without magnetic field exposure, and (F) with 200 mT exposure for 30 min daily. ∗Indicates a significant difference between each group ($p < 0.05$).

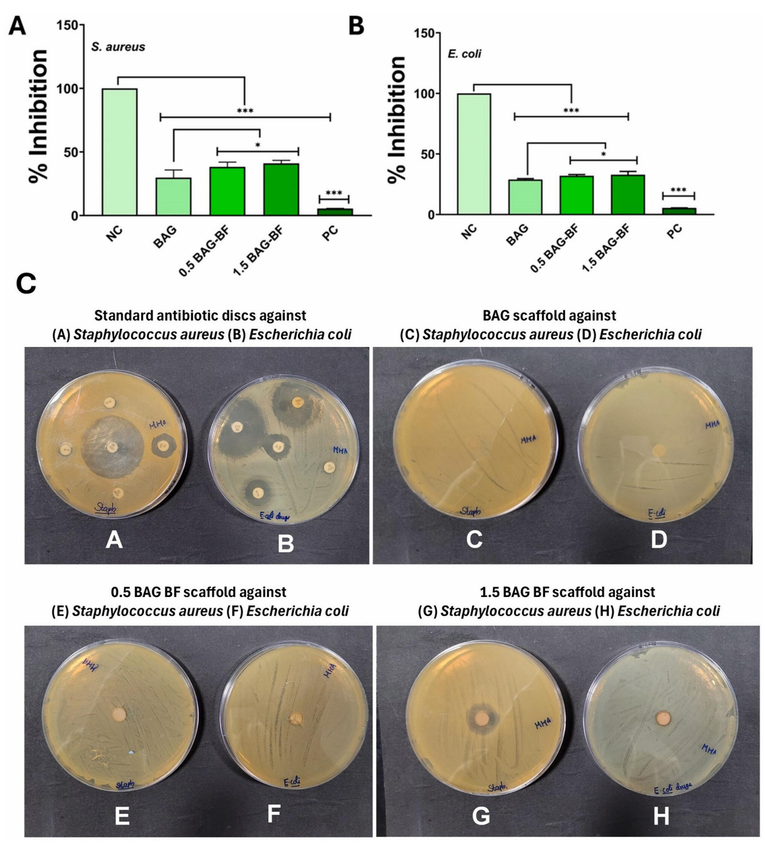


Fig. 8. Antibacterial activity of different samples against *S. aureus* and *E. coli*. The LB broth (negative control/NCs) showed nearly 100 % growth inhibition, while BAG exhibited significantly lower inhibition ($p < 0.001$) (A and B). Both 0.5 BAG-BF and 1.5 BAG-BF showed higher inhibition than BAG, with no significant difference ($p < 0.05$ for *E. coli* and $p < 0.001$ for *S. aureus*). (C) Antimicrobial activity of scaffolds assessed by the Kirby-Bauer method. BAG and 0.5 BAG-BF showed no measurable antibacterial effect, while 1.5 BAG-BF exhibited a prominent zone of inhibition against S. aureus (<2 cm).

MTT assays demonstrated significantly enhanced proliferation of MC3T3-E1 pre-osteoblast cells on BAG-BF composites compared to pure BAG and tissue culture polystyrene controls. Notably, under a 200 mT magnetic field, the 1.5 wt% BAG-BF scaffolds exhibited the highest proliferation, reaching approximately 185% by day 5, highlighting the synergistic effect of BF-induced magneto-electric stimulation. Mild hemolytic activity (<5%) was observed for all scaffolds, increasing slightly with BF content but remaining within acceptable limits for biomaterials.

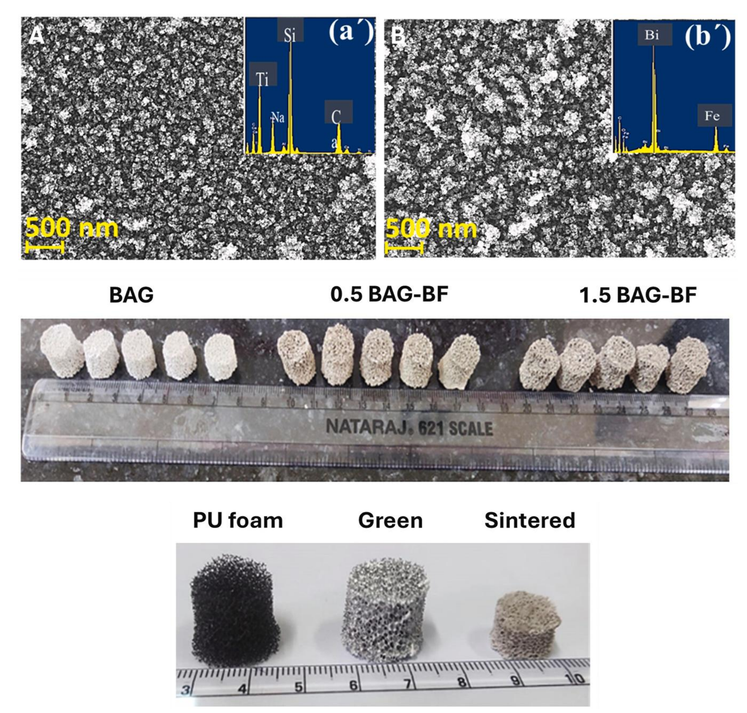


Fig. 3. The FESEM images of (A) pure BAG and (B) BF powder, along with their respective EDAX profiles (a') and (b'), are presented. (C) Typical PU foam along with green and sintered scaffolds.

Antibacterial testing showed that both BAG-BF compositions provided greater bacterial growth inhibition than pure BAG against *S. aureus* and *E. coli*, with the 1.5 wt% BAG-BF scaffolds exhibiting a measurable zone of inhibition against *S. aureus*.

CONCLUSIONS

This study demonstrated that BF-BAG scaffolds significantly improve mechanical strength, bioactivity, and cell proliferation, making them promising candidates for bone tissue regeneration. They exhibited porosities of ~74 % (BAG), ~65 % (0.5 BAG-BF), and ~64 % (1.5 BAG-BF), with ~50 % shrinkage and post-sintering weight losses of 5 %, 2.5 %, and 5 %, respectively. Bismuth ferrite incorporation enhanced compressive strength, with 0.5 BAG-BF (1.81 MPa, ~29 % increase) and 1.5 BAG-BF (1.87 MPa, ~33 % increase) compared to pure BAG (1.45 MPa). The 1.5 BAG-BF scaffold exhibited enhanced bioactivity and mild antibacterial properties, although its hemolytic effect warrants caution. These findings highlight the potential of BAG-BF scaffolds for bone regeneration while emphasizing the need for further evaluation of their biocompatibility. BF-incorporated BAG scaffolds show great potential but require additional refinement for safe and effective clinical application.

REFERENCES

Banu SA, Rahaman SH, Sharun K, Mamachan M, Maiti SK, Bodhak S, Balla VK, Pawde AM. Bismuth ferrite reinforced porous bioactive glass scaffolds: *In vitro* and antibacterial properties. Heliyon. 2025 Jul 1;11(12).

Banu SA, Sharun K, Mamachan M, Rahaman SH, Deekshitha V, Karikalan M, Sharma GK, Vinodkumar OR, Maiti SK, Bodhak S, Balla VK. Multiferroic Bioactive Glass Biocomposites and Magnetic Stimulation Accelerate Rat Calvarial Bone Regeneration. Journal of Drug Delivery Science and Technology. 2026 Mar 23:108272.

Khatua C, Bhattacharya D, Kundu B, Balla VK, Bodhak S, Goswami S. Multiferroic reinforced bioactive glass composites for bone tissue engineering applications. Advanced Engineering Materials. 2018 Dec;20(12):1800329.

Khatua C, Bodhak S, Kundu B, Balla VK. *In vitro* bioactivity and bone mineralization of bismuth ferrite reinforced bioactive glass composites. Materialia. 2018 Dec 1;4:361-6.

Rahaman SH, Bodhak S, Balla VK, Bhattacharya D. Role of in-situ electrical stimulation on early-stage mineralization and in-vitro osteogenesis of electroactive bioactive glass composites. Biomaterials Advances. 2025 Jan 1;166:214062.

Questions?
SCAN TO CONNECT

KEY POINTS

- Adding bismuth ferrite to bioactive glass increased compressive strength compared to pure BAG, while retaining high porosity suitable for bone tissue engineering.
- BF-reinforced scaffolds significantly promoted pre-osteoblast cell growth, with the highest proliferation observed for 1.5 wt% BF under a 200 mT magnetic field
- The foam-replicated scaffolds exhibited highly interconnected porosity (64–74%) and pore sizes of ~400–500 µm, ideal for nutrient diffusion, vascularization, and bone ingrowth.
- The 1.5 wt% BF scaffold showed mild intrinsic antibacterial activity against *S. aureus* while maintaining hemolysis below 5%.

ACKNOWLEDGEMENTS

The authors acknowledge all funding agencies and supporting institutions.

AALBORG UNIVERSITY | DEPARTMENT OF HEALTH SCIENCE AND TECHNOLOGY

CGCRI CECRI कर्मणेव हि संसिद्धिम्
IVRI
सत्यमेव जयते
विज्ञान एवं प्रौद्योगिकी मंत्रालय MINISTRY OF SCIENCE AND TECHNOLOGY
भाकृअनुप ICAR
iNSERB DIA
termis EUROPE
Orthoregeneration Network